

# Incorporating model uncertainty in collapse reliability assessment of buildings

B. Ugurhan, J.W. Baker & G.G. Deierlein

*Department of Civil and Environmental Engineering, Stanford University*

**ABSTRACT:** Structural collapse analysis requires models that capture large deformation response with cyclic strength and stiffness degradation. Although current collapse assessment methods carefully account for the nonlinear response of structures, most of these analyses are conducted with models that reflect the median (or expected) properties of the structural components and do not fully account for model uncertainties associated with variability in the properties and response characteristics of the components. This work discusses several advances in treatment of model uncertainty for collapse safety assessment. A variety of reliability methods are explored and compared to evaluate their ability to characterize accurately the influence of modeling uncertainties and variability in component behavior on overall system response. The examples serve as illustrations of approaches to rigorously assess the influence of model uncertainties and variability in component properties on the collapse behavior of the systems.

## 1 INTRODUCTION

Seismic design provisions in building codes aim to provide adequate collapse safety of structures even in extreme events. Collapse response of structures is characterized by highly nonlinear behavior of its components and its assessment requires nonlinear analysis models that capture large inelastic deformations with significant cyclic strength and stiffness degradation. In addition, for comprehensive assessment of collapse, uncertainties coming from various sources at component level should be characterized and propagated in a probabilistic framework through a system reliability approach. The sources of uncertainties can be listed as the variability in ground motion and structural response simulations. The uncertainty in structural response simulations can be due to design and modeling of the structure. Different structural idealizations ranging from phenomenological models to finite element discretizations capture certain modes of failure. This brings uncertainty in terms of utilizing different analysis methods and different definitions of analysis model parameters. Model parameters are also subject to uncertainty. Conducting structural analysis with the median (or expected) values of the model parameters do not account for the variability in the properties and the response characteristics of structural components.

Using a probabilistic collapse response assessment approach, this study aims to assess the effects

of model parameter uncertainties on structural collapse safety. Correlations of random variables play a significant role in uncertainty propagation. Accurate assessment of modeling uncertainty in terms of collapse response requires reliable estimations of correlations of model parameters within and between components in a structure.

An early attempt to assess the effects of uncertainties in modeling parameters on collapse response is done by Ibarra & Krawinkler (2003), in which they show that post-yield stiffness and ductility capacity are the parameters most affecting collapse response. Later, Haselton (2006) quantified and propagated the uncertainties using the First-Order Second-Moment (FOSM) approximation. Vamvatsikos & Fragiadakis (2009) and Dolsek (2009) used Monte Carlo simulation with Latin-Hypercube sampling to assess the effects of uncertainties in model parameters on collapse response of structures.

Rajasheshkar & Ellingwood (1993) utilized response surface method to approximate limit state functions in structural reliability problems whereas Papadrakakis et al. (1996) used artificial neural networks (ANN) to compute probability of failure of elastoplastic structures. Dengi et al. (2005) combined ANNs with structural reliability methods to estimate limit state functions and the partial derivatives. Liel et al. (2009) with a robust nonlinear structural model used the response surface approach to predict collapse response which incorporates ground motion and modeling uncertainties. This study

builds on the findings of Liel et al. (2009). We aim to assess the effects of modeling uncertainties on collapse response with emphasis on quantifying correlation of model parameters. Alternative reliability methods to assess the effects of modeling uncertainty in collapse response assessment are also investigated.

## 2 COLLAPSE ASSESSMENT PROCEDURE

Collapse simulation of structures requires numerical models that can reproduce the nonlinear deformation demands and degradation in stiffness and strength in the elements due to repeated cycles of loading. The component hinge model originally developed by Ibarra et al. (2005) is capable of simulating nonlinear hysteretic behavior of reinforced concrete (RC) beam-column elements. It is based on a tri-linear monotonic backbone curve, relating member moment and rotation, along with nonlinear hysteretic rules to simulate strength and stiffness degradation under cyclic loading. The strength of this model in collapse simulation is due to the post-capping branch that is characterized by a negative slope. This portion of the backbone curve simulates strain-softening behavior related to concrete crushing, rebar fracture and buckling. The accuracy of the simulation depends on realistic characterization of parameters of the phenomenological model. Therefore, in this study we assume six parameters defining the backbone curve, namely  $\theta_y$ ,  $M_y$ ,  $\theta_{cap,pl}$ ,  $M_c/M_y$ ,  $\theta_{pc}$  and  $\gamma$  are random variables. An example backbone curve displaying model parameters is provided in Figure 1.

Incremental dynamic analysis (IDA) is a fairly established technique used to predict collapse (Vamvatsikos & Cornell 2002). In this technique nonlinear response history analysis is conducted using a ground motion that is scaled to various intensity levels. Collapse intensity is estimated as the intensity level that causes dynamic instability. This procedure is repeated for a number of ground motions. Different ground motions cause collapse at different ground motion intensities, producing rec-

ord-to-record variability in collapse capacities. To account for record-to-record variability, 22 ground motion record pairs from the FEMA-P695 (FEMA 2009) far-field ground motion set are used in this study. The data set is selected such that it consists of extreme motions that may cause structural collapse. In this study, incremental dynamic analysis with a component hinge model is used for collapse assessment with the OpenSees analysis platform.

## 3 BRIDGE COLUMN MODEL

A reinforced concrete bridge column that was tested full-scale in NEES Outdoor Shake Table at UCSD in 2010 (PEER & NEES 2010) is used as a case study structure for the assessment of modeling uncertainties. The bridge column is designed according to Caltrans Seismic Design Criteria and Bridge Design Specifications (Caltrans 2004, 2006) and seismic performance of bridge columns built in compliance with current U.S. standards is aimed to be investigated.

The circular column has a diameter of 4 ft (1.2 m) and height of 24 ft (7.2 m). To mobilize the column capacity, a 250 ton (2,245 kN) reinforced concrete block was cast on top of the column (Terzic et al. 2012).

The bridge column is modeled as a single degree of freedom structure with a concentrated hinge model defined at the base. The first mode period of the structure ( $T_1$ ) is obtained as 1.11 sec. The backbone curve parameters for the bridge column model have been calibrated using experimental results and the calibrated parameters are assumed to reflect median properties. The bridge column is observed to be highly ductile having a ductility capacity of 6.45.

## 4 ASSESSMENT OF CORRELATION OF MODEL PARAMETERS BETWEEN AND WITHIN COMPONENTS

Haselton et al. (2008) calibrated the concentrated plastic hinge model by Ibarra et al. (2005) to represent nonlinear hysteretic behavior of reinforced concrete (RC) beam-columns. The component calibration database consists of 255 tests of rectangular RC columns that failed either in flexure or in combined flexure-shear mode (Berry et al. 2004, Haselton 2008). The database consists of 42 test groups. A test group refers to a set of tests conducted by one researcher. The number of tests per group range between 1 and 24. Haselton et al. used the database to calibrate empirical predictive equations for the backbone curve parameters. The predictive equations for  $\theta_{pc}$ ,  $\theta_{cap,pl}$ ,  $M_c/M_y$  and  $\gamma$  are reported in

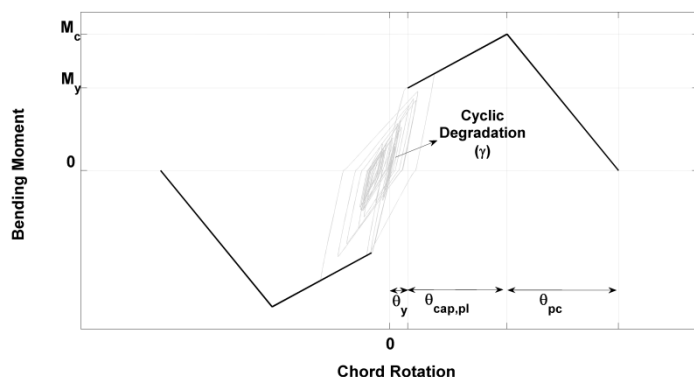


Figure 1. Backbone Curve of the Component Hinge Model.

Haselton et al. (2008). Readers are referred to Panagiotakos & Fardis (2001) for equations regarding  $\theta_y$  and  $M_y$ . The goodness of fit of the predictive equations is investigated through residuals which are defined using the below equation:

$$\ln RV_{ij} = \ln (Prediction_{RV_{ij}}) + \varepsilon_{ij} \quad (1)$$

where  $\ln RV_{ij}$  represents the logarithm of the observed value of the random variable,  $RV$ , for test  $j$  of the  $i^{\text{th}}$  test group,  $Prediction_{RV_{ij}}$  is the predicted value for the random variable and  $\varepsilon_{ij}$  is the residual having a mean of zero and standard deviation of  $\sigma$ . Haselton et al. (2008) also reported the median, mean and standard deviation of residuals associated with the calibrated tests.

The correlations within component model parameters are computed using Pearson's product-moment correlation coefficient between residuals of the random variables and are displayed in Table 1:

Table 1. Correlation coefficients within component model parameters.

	$\theta_y$	$M_y$	$M_c/M_y$	$\theta_{\text{cap,pl}}$	$\theta_{\text{pc}}$	$\gamma$
$\theta_y$	1.0	0.6	0.4	0.1	0.5	0.2
$M_y$		1.0	0.3	0.1	0.2	0.1
$M_c/M_y$			1.0	0.3	0.2	0.2
$\theta_{\text{cap,pl}}$				1.0	0.2	0.1
$\theta_{\text{pc}}$					1.0	0.4
$\gamma$						1.0

(symmetric)

Assessment of correlation of model parameters between components is important to capture interactions between different components of a system and accurately estimate of system failure probabilities. We assume that correlations among the sets of experiments conducted by different test groups give an estimation of the correlations between component in a structure. In Figure 2, all pairs of residuals obtained from Equation 1 for tests within the same test group are plotted for each model parameter. Within each plot, each test group is represented with a specific color and symbol combination.

Among the six plots, the  $M_y$  and  $\theta_y$  data show strong grouping of residuals by test group. This suggests that all of the  $M_y$  and  $\theta_y$  values observed in a given test group tend to have similar variation away from their corresponding predictions. The observed grouping suggests that the parameter uncertainty of  $\theta_y$  and  $M_y$  in the building's components has significant correlation from one component to another. To quantify these effects, two-way mixed effects regression analysis is utilized (Pinheiro & Bates, 2000). In mixed effects regression, the residual  $\varepsilon_{ij}$  of Equation 1 is further grouped to take into account factors related to fixed and random effects terms. Thus, it is written as:

$$\ln RV_{kij} = \ln (Prediction_{RV_{kij}}) + \alpha_k + \beta_i + \gamma_j + (\alpha\beta)_{ki} + (\beta\gamma)_{ij} + \xi_{kij} \quad (2)$$

In the above equation, indices  $k$ ,  $i$  and  $j$  refer to the random variable of interest, test group and test number, respectively. It is assumed that  $\alpha_k$  is normally distributed with a mean of zero and standard deviation of  $\sigma_\alpha$ , i.e.  $\alpha_k \sim N(0, \sigma_\alpha^2)$ . Using the similar

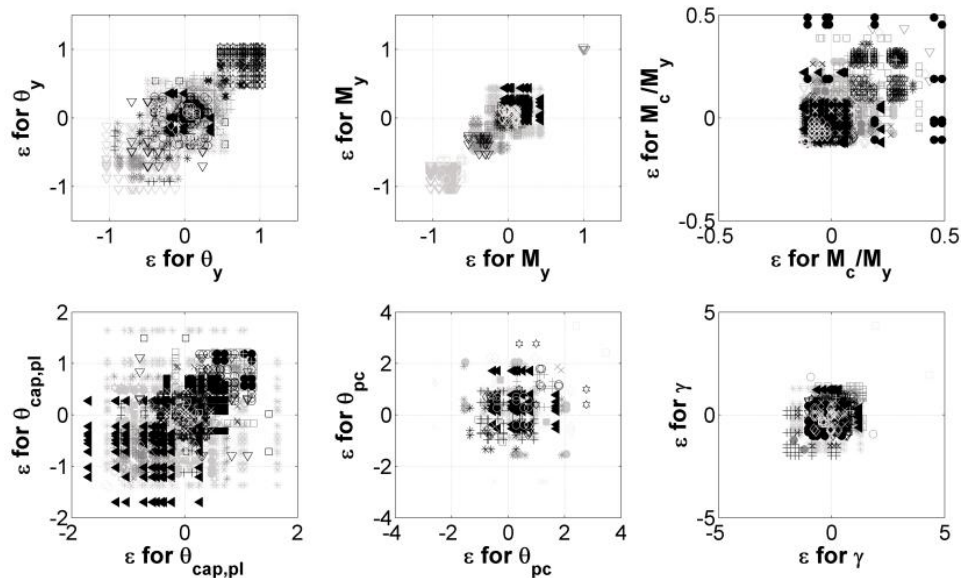


Figure 2. Residuals between observed and predicted values for each random variable.

Table 2. Correlation coefficients of model parameters between and within components. Using the notation in Equation 2, correlation coefficients are given for  $j=1$  and 2.

		COMPONENT $j=1$						COMPONENT $j=2$					
		$\theta_{y1}$	$M_{y1}$	$M_c/M_{y1}$	$\theta_{cap,pl1}$	$\theta_{pc1}$	$\gamma_1$	$\theta_{y2}$	$M_{y2}$	$M_c/M_{y2}$	$\theta_{cap,pl2}$	$\theta_{pc2}$	$\gamma_2$
COMPONENT $j=1$	$\theta_{y1}$	1.0	0.4	0.1	0.1	0.4	0.2	0.7	0.3	0.1	0.1	0.3	0.2
	$M_{y1}$		1.0	0.3	0.1	0.1	0.1	0.3	0.9	0.3	0.1	0.0	0.1
	$M_c/M_{y1}$			1.0	0.1	0.0	0.0	0.1	0.3	0.6	0.1	0.0	0.0
	$\theta_{cap,pl1}$				1.0	0.1	0.1	0.1	0.1	0.1	0.4	0.0	0.0
	$\theta_{pc1}$					1.0	0.4	0.3	0.0	0.0	0.0	0.2	0.3
	$\gamma_1$						1.0	0.2	0.1	0.0	0.0	0.3	0.5
COMPONENT $j=2$	$\theta_{y2}$	(symmetric)						1.0	0.4	0.1	0.1	0.4	0.2
	$M_{y2}$								1.0	0.3	0.1	0.1	0.1
	$M_c/M_{y2}$									1.0	0.1	0.0	0.0
	$\theta_{cap,pl2}$										1.0	0.1	0.1
	$\theta_{pc2}$											1.0	0.4
	$\gamma_2$												1.0

notation,  $\beta_i \sim N(0, \sigma_\beta^2)$ ,  $\gamma_j \sim N(0, \sigma_\gamma^2)$ ,  $(\alpha\beta)_{ki} \sim N(0, \sigma_{\alpha\beta}^2)$ ,  $(\beta\gamma)_{ij} \sim N(0, \sigma_{\beta\gamma}^2)$  and  $\check{\epsilon}_{kij} \sim N(0, \sigma^2)$ . It is noted that the standard deviations are obtained using the regression model defined by Equation 2. Given the model of Equation 2, correlation coefficients is obtained using Equations 3,4 and 5.

$$\rho_{RV_{kij}, RV_{k'ij}} = \frac{\sigma_\beta^2 + \sigma_\gamma^2 + \sigma_{\beta\gamma}^2}{\sigma_\alpha^2 + \sigma_\beta^2 + \sigma_\gamma^2 + \sigma_{\alpha\beta}^2 + \sigma_{\beta\gamma}^2 + \sigma^2} \quad (3)$$

In Equation 3,  $k$  and  $k'$  represent different random variables and  $\rho_{RV_{kij}, RV_{k'ij}}$  reflects the correlation between random variables,  $k$  and  $k'$ , in one component of a structure, i.e.  $j^{\text{th}}$  component in  $i^{\text{th}}$  structure.

$$\rho_{RV_{kij}, RV_{k'ij'}} = \frac{\sigma_\alpha^2 + \sigma_\beta^2 + \sigma_{\alpha\beta}^2}{\sigma_\alpha^2 + \sigma_\beta^2 + \sigma_\gamma^2 + \sigma_{\alpha\beta}^2 + \sigma_{\beta\gamma}^2 + \sigma^2} \quad (4)$$

In Equation 4,  $j$  and  $j'$  represent different components in a structure and  $\rho_{RV_{kij}, RV_{k'ij'}}$  is the correlation of a random variable,  $k$ , between different components of the  $i^{\text{th}}$  structure.

$$\rho_{RV_{kij}, RV_{k'ij'}} = \frac{\sigma_\beta^2}{\sigma_\alpha^2 + \sigma_\beta^2 + \sigma_\gamma^2 + \sigma_{\alpha\beta}^2 + \sigma_{\beta\gamma}^2 + \sigma^2} \quad (5)$$

In Equation 5,  $\rho_{RV_{kij}, RV_{k'ij'}}$  is assumed to reflect the correlation between random variables,  $k$  and  $k'$ , of different components of a structure, i.e. components  $j$  and  $j'$  of structure  $i$ .

Table 2 shows the correlation coefficients obtained using the aforementioned approaches. These correlation coefficients are utilized in assessing collapse safety of frame structures. It is noted that using different approaches resulted in different correlation coefficients of model parameters within components.

## 5 MODELING UNCERTAINTY ASSESSMENT OF AN EXAMPLE BRIDGE COLUMN

Using the FEMA-P695 far field record set, incremental dynamic analysis is performed on the bridge column. The backbone curve of the bridge column is calibrated using experimental results and the calibrated parameters are assumed to be median component parameters. IDA curves for the median model are displayed in Figure 3a.

To assess modeling uncertainty, a Monte Carlo (MC) approach is utilized. 250 realizations of component model parameters are obtained using a multivariate normal joint distribution of the parameters. To simulate realizations of component model parameters having a multivariate joint distribution of parameters, mean, standard deviation and correlation coefficients of random variables are needed. As mentioned previously, the calibrated parameters are assumed to be median component parameters. The logarithmic standard deviations ( $\sigma_{ln}$ ) for  $\theta_{pc}$ ,  $\gamma$ ,  $\theta_{cap,pl}$  and  $M_c/M_y$  are reported in Haselton et al. (2008) as 0.86, 0.64, 0.63 and 0.13, respectively. For  $\theta_y$  and  $M_y$  using the database and the predictive equations of Panagiotakos & Fardis (2001) the dispersion values are computed as 0.43 and 0.3, respectively. Cor-

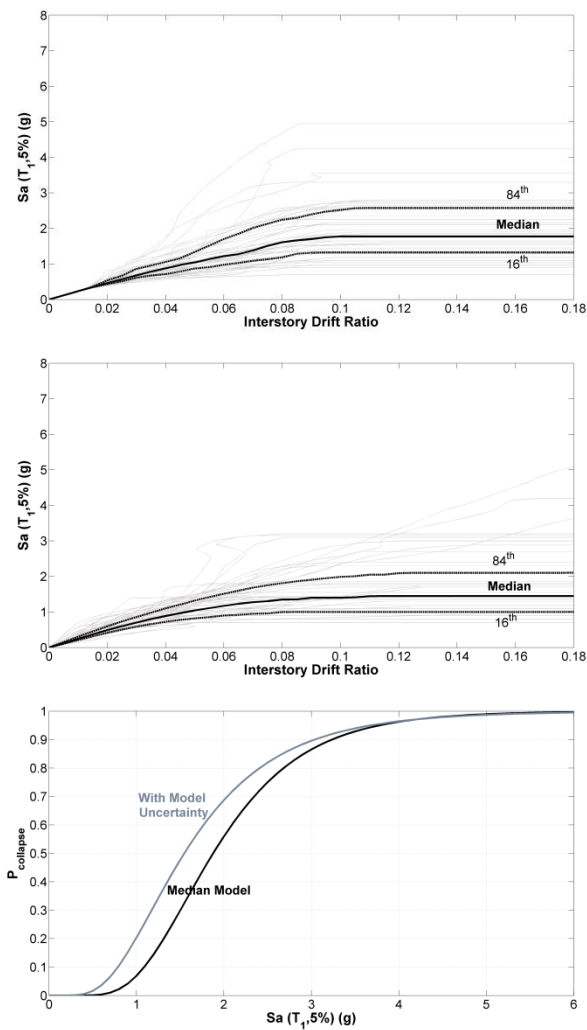


Figure 3. a) IDA curves of the median model obtained using 44 FEMA-P695 ground motions b) Randomly selected 44 IDA curves from MC Simulations c) Collapse Fragility Curves obtained using Median Model Parameters and MC Simulations of model parameters. MC Simulations are indicated as the curve with model uncertainty.

relation coefficients are used as given in Table 1. Incremental dynamic analysis is performed for MC simulations and IDA curves are displayed in Figure 3b.

Probability of collapse given a ground motion intensity measure, IM,  $P(C|Sa(T_1, 5\%))$  can be obtained using Equation 6:

$$P(C|Sa(T_1, 5\%)) = \Phi\left(\frac{\ln(Sa(T_1, 5\%)) - \mu_{\ln Sa(T_1, 5\%)}}{\sigma_{\ln Sa(T_1, 5\%)}}\right) \quad (6)$$

In Equation 6,  $\Phi(\cdot)$  is the standard normal cumulative distribution function.  $\mu_{\ln Sa(T_1, 5\%)}$  and  $\sigma_{\ln Sa(T_1, 5\%)}$  are the mean and standard deviation of  $\ln Sa(T_1, 5\%)$ , respectively.  $Sa(T_1, 5\%)$  is the spectral acceleration at the fundamental period of the structure,  $T_1=1.11$  sec and damping as 5%. Method of moments is used to compute  $\mu_{\ln Sa(T_1, 5\%)}$  and

$\sigma_{\ln Sa(T_1, 5\%)}$ . The collapse fragility curves obtained using median model parameters and MC simulations are given in Figure 3c.

By neglecting model uncertainty, it is observed that unconservative results are obtained. Incorporating modeling uncertainties caused 30% decrease in the median collapse capacity and 25% increase in dispersion of the collapse fragility curve compared to the fragility curve obtained using median model parameters.

The collapse fragility curves are integrated with the hazard curve at a representative site at Los Angeles located at  $34.00^\circ$  latitude,  $-118.16^\circ$  longitude where near fault effects are not expected to be observed (Haselton 2006). When model uncertainty is considered, the collapse rate is observed to be 3.6 times the mean annual collapse rate ( $\lambda_c$ ) of the one obtained using median properties. The intensity level corresponding to maximum considered earthquake, which is defined by 2% probability of exceedance in 50 year, is 0.73 g and at this intensity level, probability of collapse,  $P_{collapse}$ , increases from 0.5% to 5% when modeling uncertainty is taken into account.

## 6 STRUCTURAL COLLAPSE CAPACITY PREDICTION USING ALTERNATIVE METHODS

Collapse assessment of structures requires computationally intensive nonlinear response history analyses. Incorporation of uncertainties related to ground motion and structural modeling increases computational demand significantly. To practically consider modeling variability in collapse simulation, alternative predictive models are needed to estimate collapse fragility of a given structural model. In this study we present three approaches, namely First-Order Second-Moment, response surface and ANN methods.

### 6.1 First-Order Second-Moment Method (FOSM)

FOSM is a standard method to propagate uncertainties. Using a Taylor series expansion around the mean, the limit state function defining structural collapse in terms of random variables is linearized, such that the response given mean inputs is unchanged. The variance of the response is computed using the gradients of limit state function with respect to the random variables. The details of this approach can be found in Baker & Cornell (2003). Since the limit state function does not have an analytical functional form, the gradients of the

limit state function is obtained by perturbing each random variable in a series of sensitivity analyses. For this study, each variable is perturbed up to  $\pm\sqrt{3}\sigma_{ln}$  away from their means with increments of  $0.25\sigma_{ln}$  and a linear trend line is fitted in log scale to compute the two-sided derivatives. For  $M_c/M_y$  and  $\gamma$ , we observed a strong nonlinear relationship between the random variables and the collapse capacity. It is observed that the collapse capacity estimations do not increase with the increase in  $\gamma$  and  $M_c/M_y$ . Since reducing these two variables is more critical for the structure and it leads to lower collapse capacities, leftward gradient, which is obtained by perturbing the variables only in negative direction, is used for these variables in FOSM calculations.

The extreme values each random variable is assigned during FOSM calculations and their relative effect on collapse capacity estimations is displayed through a tornado diagram in Figure 4. The diagram shows the sensitivity of each model parameter with respect to the median collapse capacity. It is observed that median collapse capacity is highly sensitive to  $\theta_y$ ,  $\theta_{cap,pl}$ ,  $\theta_{pc}$  and  $M_y$ .

## 6.2 Response Surface Approach

To calibrate the predictive models of response surface and ANN approaches, design of experiments with central composite design is used (Pinto et al. 2005). Each random variable is perturbed  $\pm 1.7\sigma_{ln}$  from the mean individually, and in combinations with other random variables at  $\pm 1\sigma_{ln}$ . For the six random variables used in this study, experimental design dataset is composed of 73 combinations of these variables. For each design point, a nonlinear model is created with modified parameter values, and incremental dynamic analysis is performed with FEMA-P695 far-field ground motion set. Fragility

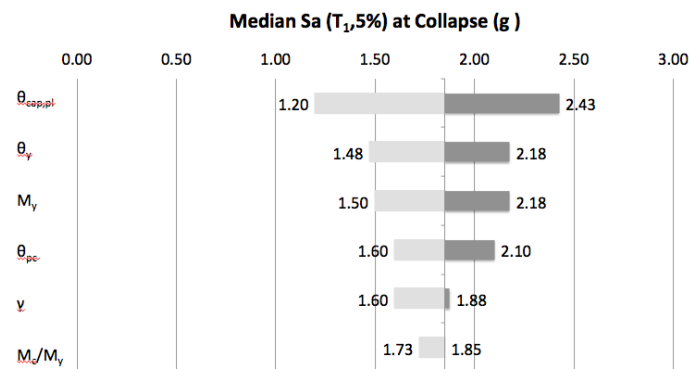


Figure 4. Tornado diagram showing the sensitivity of model parameters. Dark and light gray bars show the change in median collapse capacity when the associated random variables are perturbed  $+\sqrt{3}\sigma_{ln}$  and  $-\sqrt{3}\sigma_{ln}$ , respectively.

functions are obtained using the incremental dynamic analysis results for each nonlinear analysis model.

For response surface approach, using the experimental design set, a second-order polynomial function is fit to  $Sa(T_1, 5\%)$  values corresponding to 0.5 probability of failure. For given model parameters, response surface predicts median collapse capacity and the collapse fragility function is obtained using the median collapse capacity prediction and record-to-record variability of the median model as dispersion.

Using Monte Carlo simulation, various realizations of model parameters are then obtained and the corresponding fragility functions are predicted. For each  $Sa(T_1, 5\%)$  level, the mean of probabilities from the predicted fragility functions are obtained to compute the final fragility function, which incorporates modeling and ground motion uncertainty.

## 6.3 Artificial Neural Network Approach

For the ANN approach,  $Sa(T_1, 5\%)$  values corresponding to probabilities of 0.1 and 0.25 are obtained from the individual fragility functions of experimental design dataset. The two-point representation of the fragility function is motivated by the work of Eads et al. (2012) who proposed an efficient method where two intensity levels on a fragility function is selected such that the selected intensities contribute to collapse risk significantly. They observed that lower tail of the collapse fragility function dominates collapse risk.

The neural network uses experimental design data as the training set. In addition to the training, calibration of neural networks involves validation and testing, which increase their predictive capabilities. For validation and testing sets, new data is generated randomly having a size 15% of the experimental design dataset.

A multi-layer feed forward network is calibrated such that it outputs  $Sa(T_1, 5\%)$  values at the two probability levels, namely 0.1 and 0.25. The fragility

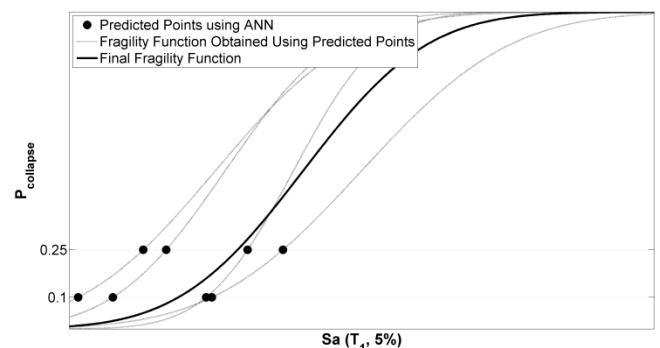


Figure 5. Illustrative figure showing ANN approach.

function is predicted by fitting through the two predicted points. For each  $Sa(T_1, 5\%)$  level, the mean of probabilities from the predicted fragility functions are obtained to yield estimation of the final fragility function, which incorporates modeling and ground motion uncertainty. Figure 5 illustrates this approach.

## 7 RESULTS

Figure 6a shows the collapse fragility functions obtained using MC simulations, ANN, response surface and FOSM methods. The collapse fragility curve obtained using ANN approach is similar to the one obtained using MC simulations. Close estimation of the MC simulation result is also obtained with the response surface method.

The number of incremental dynamic analysis conducted are 3,212, 3,740, 4,180 and 11,000 for response surface, FOSM, ANN and MC simulation approaches, respectively. Since 44 ground motions are used for each structural model, the number of different structural models used are 73, 85, 95 and 250 for response surface, FOSM, ANN and MC simulation approaches, respectively. The computational demand for response surface and ANN is similar. Although FOSM have comparable number of analysis with response surface and ANN, it is possible to conduct FOSM with only 7 structural models.

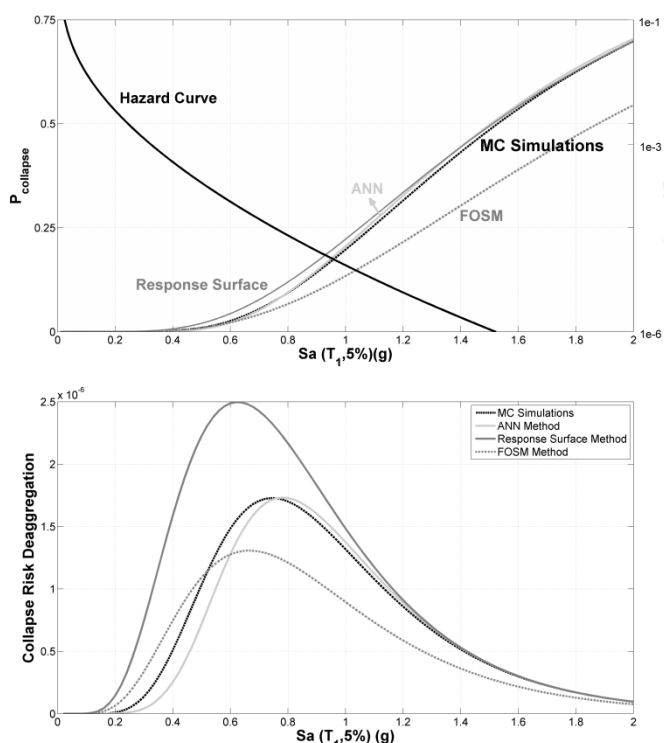


Figure 6. a) Collapse fragility functions and hazard curve at a representative site at Los Angeles b) Collapse risk deaggregation curves obtained using MC Simulation, FOSM, ANN and Response Surface approaches.

85 different models are used in this study to increase the confidence in gradient computations. For MC simulations, there is a trade-off between the number of simulations conducted and the level of accuracy in the computations. One can reduce the number of MC simulations; however the variability in the results increases.

Response surface and ANN approaches can capture nonlinear relationships between the random variables and collapse capacity, whereas FOSM is not capable of capturing the nonlinear relations. From Figure 3c, we observed that incorporating modeling uncertainties increases the dispersion in collapse fragility function and shifts the median collapse capacities to the left. As discussed in Section 6.1, using a Taylor series expansion around the mean, FOSM is not able to reproduce the shift in the median collapse capacity; whereas other methods are observed to catch this behavior.

Also indicated in Figure 6a is the hazard curve at the representative site at Los Angeles. At each  $Sa(T_1, 5\%)$  level, the collapse fragility functions are multiplied with the slope of the hazard curve to obtain collapse risk deaggregation curves (Eads et al. 2012) given in Figure 6b. The area under a collapse risk deaggregation curve gives  $\lambda_c$  and the curve identifies the ground motion intensities that contribute most to  $\lambda_c$ . It is observed that for this structure, ground motions with  $Sa(T_1, 5\%) = 0.75$  g contribute most to the collapse risk. ANN approach provided good predictions both in terms of collapse fragility function and  $\lambda_c$ . Although response surface approach predicts the overall collapse fragility curve sufficiently, the misfit in the lower tail of the distribution resulted in overestimation of  $\lambda_c$  by 40%. On the other hand, although the collapse fragility curve predicted by FOSM was far-off, the underestimation in  $\lambda_c$  is 20%.

## 8 CONCLUSIONS

In this study, we assessed the effects of modeling uncertainty in the collapse response of a bridge column. For the random variables defining the analysis model, correlation coefficients are quantified by the statistical analysis of calibration database of Haselton et al. (2008). Correlations are investigated both between multiple parameters for a single component and between parameters for various components in a building. Two approaches are utilized to assess correlations in a structure. As the first approach, Pearson's product-moment correlation coefficients are computed which reflect correlations of model parameters within components. The second approach utilizes two-way mixed effects regression,

which resulted in correlation of model parameters both between and within components. Using the correlation coefficients and the multivariate distribution of the random variables, modeling uncertainty in the collapse response of a bridge column is assessed. It is observed that using median model parameters in collapse risk assessment and not incorporating of modeling uncertainties leads to unconservative results. The collapse risk and the probability of collapse at a given intensity level is underestimated especially at the intensities corresponding to the lower tail of the collapse fragility function. To decrease computational demand in the probabilistic collapse analysis, alternative methods are explored to predict collapse capacity. These methods include FOSM, response surface and ANN methods. It is observed that response surface and ANN methods by capturing the nonlinear relationship between model parameters and collapse capacity provided good estimations of the overall collapse fragility curve. FOSM, on the other hand, is observed to be limited in estimating collapse fragility curve. However, the mean annual frequency of collapse prediction by FOSM is observed to be comparable to the complex response surface prediction. ANN approach gives good estimations of both collapse fragility curve and the mean annual frequency of exceedance.

## ACKNOWLEDGEMENTS

This project is financially supported by NSF CMMI-1031722. Any opinions, findings and conclusions or recommendations expressed in this material are those of the authors and do not necessarily reflect the views of the National Science Foundation.

## REFERENCES

- Baker, J. & Cornell, C. A. 2003. Uncertainty Specification and Propagation for Loss Estimation Using FOSM Methods. *PEER Report 2003/07, Pacific Engineering Research Center, University of California, Berkeley, California.*
- Berry, M., Parrish, M., & Eberhard, M. 2004. PEER Structural Performance Database User's Manual, Pacific Engineering Research Center, University of California, Berkeley, California. Available at <http://nisee.berkeley.edu/spd/> (last accessed March 2013).
- Caltrans 2004. Bridge design specifications. *California Department of Transportation, Sacramento, California, USA.*
- Caltrans 2006. Seismic Design Criteria. *California Department of Transportation, Sacramento, California, USA.*
- Dolsek M. 2009. Incremental dynamic analysis with consideration of modelling uncertainties. *Earthquake Engineering and Structural Dynamics* 38(6): 805–825.
- Eads, L., Miranda, E., Krawinkler, H. & Lignos, D. G. 2012. An efficient method for estimating the collapse risk of structures in seismic regions. *Earthquake Engineering & Structural Dynamics* doi:10.1002/eqe.2191.
- Federal Emergency Management Agency (FEMA). 2009. FEMA P695 Recommended Methodology for Quantification of Building System Performance and Response Parameters, Project ATC-63, Prepared by the Applied Technology Council, Redwood City, CA.
- Deng, J., Gu, D., Li, X. & Yue, Z.Q. 2005. Structural reliability analysis for implicit performance functions using artificial neural network, *Structural Safety* 27(1): 25–48.
- Haselton, C.B. 2006. Assessing seismic collapse safety of modern reinforced concrete frame buildings. *Ph.D. thesis, Stanford University.*
- Haselton, C.B. 2008. Reinforced Concrete Column Calibration Database. [http://myweb.csuchico.edu/~chaselton/research/research\\_databases/rc\\_db.php](http://myweb.csuchico.edu/~chaselton/research/research_databases/rc_db.php), (last accessed March 2013).
- Haselton, C.B., Liel, A.B., Lange, S.T. & Deierlein, G.G. 2008. Beam-Column Element Model Calibrated for Predicting Flexural Response Leading to Global Collapse of RC Frame Buildings, *PEER Report 2007/03, Pacific Engineering Research Center, University of California, Berkeley, California.*
- Ibarra, L. & Krawinkler, H. 2003. Global collapse of frame structures under seismic excitations. *Blume Center TR 152, Stanford University; 2003.*
- Ibarra, L.F., Medina, R.A. & Krawinkler, H. 2005. Hysteretic models that incorporate strength and stiffness deterioration. *Earthquake Engineering and Structural Dynamics* 34(12): 1489–1511.
- Liel, A.B., Haselton, C.B., Deierlein G.G. & Baker, J.W. 2009. Incorporating modeling uncertainties in the assessment of seismic collapse risk of buildings. *Structural Safety* 31(2): 197–211.
- Rajashekhar, M.R. & Ellingwood, B.R. 1993. A new look at the response surface approach for reliability analysis. *Structural Safety* 12(3): 205–220.
- Papadrakakis, M., Papadopoulos, V. & Lagaros, N.D. 1996. Structural reliability analysis of elastic-plastic structures using neural networks and Monte Carlo simulation. *Computer Methods in Applied Mechanics and Engineering* 191: 3491–3507.
- Panagiotakos, T. B. & Fardis, M. N. 2001. Deformations of Reinforced Concrete at Yielding and Ultimate. *ACI Structural Journal*, 98(2): 135–147.
- PEER & NEES 2010. Concrete Column Blind Prediction Contest. Pacific Earthquake Engineering Center and George E. Brown, Jr. Network for Earthquake Engineering Simulation, [http://nisee2.berkeley.edu/peer/prediction\\_contest/](http://nisee2.berkeley.edu/peer/prediction_contest/), (last accessed March 2013).
- Pinheiro, J. C., & Bates, D. M. 2000. *Mixed effects models in S and S-PLUS*. Springer Verlag.
- Pinto, P., Giannini, R. & Franchin, P. 2005. *Seismic Reliability Analysis of Structures*. Pavia, Italy, IUSS Press.
- Terzic V., Schoettler M. & Mahin, S. 2012. Uncertainty In Modeling Seismic Response Of Reinforced Concrete Bridge Columns, *Proceedings of 9th International Conference on Urban Earthquake Engineering and 4th Asia Conference on Earthquake Engineering.*
- Vamvatsikos, D. & Cornell, C.A. 2002. Incremental dynamic analysis. *Earthquake Engineering and Structural Dynamics* 31(3): 491–514.
- Vamvatsikos, D. & Fragiadakis, M. 2009. Incremental dynamic analysis for estimating seismic performance sensitivity and uncertainty. *Earthquake Engineering & Structural Dynamics* 39: 141–163.